


# Effective expression of Drebrin in hippocampus improves cognitive function and alleviates lesions of Alzheimer's disease in APP (swe)/PS1 ( $\Delta$ E9) mice

Yan Liu  | Yan-Feng Xu | Ling Zhang | Lan Huang | Pin Yu | Hua Zhu | Wei Deng | Chuan Qin

Comparative Medicine Centre, Peking Union Medical College (PUMC) and Institute of Laboratory Animal Sciences, Chinese Academy of Medical Sciences (CAMS), Beijing, China

## Correspondence

Chuan Qin, Comparative Medicine Centre, Peking Union Medical College (PUMC) and Institute of Laboratory Animal Sciences, Chinese Academy of Medical Sciences (CAMS), Beijing, China.  
Email: qinchuan@pumc.edu.cn

## Funding information

CAMS Innovation Fund for Medical Sciences (CIFMS): Chuan Qin major collaborative innovation project, China, Grant/Award Number: 2016-12M-2-006

## Summary

**Aims:** Alzheimer's disease (AD), a progressive development dementia, is increasingly impacting patients' living conditions worldwide. Despite medical care and funding support, there are still no highly individualized drugs and practical strategies for clinical prevention and treatment. Developmentally regulated brain protein (abbreviated as Drebrin or Dbn, also known as Dbn1 in mouse) exists in neurons, especially in dendrites, and is an actin-binding protein that modulates synaptic morphology and long-term memory. However, the majority of previous studies have focused on its upstream proteins and neglected the impact Drebrin has on behavior and AD in vivo.

**Methods:** Here, we tracked the behavioral performances of 4-, 8-, 12-, and 16-month-old AD mice and investigated the expression level of Drebrin in their hippocampi. A Pearson correlation analysis between Drebrin levels and behavioral data was performed. Subsequently, 2-month-old AD mice were injected with rAAV-zsGreen-Dbn1 vector, composing the APP/PS1-Dbn1 group, and sex- and age-matched AD mice were injected with rAAV-tdTomato vector to serve as the control group. All mice were conducted behavioral tests and molecular detection 6 months later.

**Results:** (i) The expression of Drebrin is decreased in the hippocampus of aged AD mice compared with that of age-matched WT and young adult AD mice; (ii) cognitive ability of APP/PS1 mice decreases with age; (iii) Drebrin protein expression in the hippocampus correlates with behavioral performance in different aged AD mice; (iv) cognitive ability improved significantly in APP/PS1-Dbn1 mice; (v) the expression level of Drebrin in APP/PS1-Dbn1 mouse hippocampus was significantly increased; (vi) the pathological lesion of AD was alleviated in APP/PS1-Dbn1 mice; (vii) the filamentous actin (F-actin) and microtubule-associated protein 2 (MAP-2) in APP/PS1-Dbn1 mice were notably more than control mice.

**Conclusion:** In this study, an effective expression of Drebrin improves cognitive abilities and alleviates lesions in an AD mouse model. These results may provide some valid resources for therapy and research of AD.

## KEYWORDS

Alzheimer's disease, APP (swe)/PS1 ( $\Delta$ E9) mice, behavior, Drebrin, hippocampus

## 1 | INTRODUCTION

Alzheimer's disease (AD) is a type of degenerative disease with latent clinical characteristics in its early stage. It is an age-related dementia with multiple symptoms, including amnesia, disorientation, aphasia, and agnosia.<sup>1-3</sup> AD has increasingly impacted patients' living quality and places an immense burden on families. With an increasing aging population, the rising incidence of AD patients has caused an increase in medical costs and mortality in patients over 65 years of age.<sup>4,5</sup> The main pathological characteristics of AD are senile plaques (SP) that derive from deposits of amyloid  $\beta$  ( $A\beta$ )-peptide and neurofibrillary tangles (NFT), which result from the abnormal phosphorylated microtubule-associated protein tau. These pathologies contribute to the final outcome of neuronal and synaptic death.<sup>6-9</sup> However, synaptic linkage is the foundation of information transmission between neurons at the distal ends of dendrites, and changes to this transmission play an important role in memory.<sup>10,11</sup> Furthermore, learning and memory impairment observed in AD has a close relationship with hippocampal synaptic damage in its early stage.<sup>12,13</sup> Developmentally regulated brain protein (abbreviated as Drebrin or Dbn, also known as Dbn1 in mouse) is distributed in the cytoplasm of neurons, especially in the synapse. It can combine with filamentous actin (F-actin) in the postsynaptic density (PSD) to maintain long-term potentiation (LTP) in the hippocampus. Drebrin plays an important role in long-term memory<sup>14,15</sup> and regulates memory activities by combining with or depolymerizing F-actin.<sup>16-18</sup> In addition, Drebrin also plays a pivotal role in cell migration, synaptogenesis, and synaptic plasticity.<sup>19,20</sup> Postmortem studies show that Drebrin in the frontal cortex and hippocampus of AD patient brains is significantly lower than in normal brains.<sup>21,22</sup> This implies that low levels of Drebrin may play a vital role in the clinical and pathological manifestations of AD.

The majority of the studies on Drebrin were conducted on a molecular and cellular level to explore its structure and function. Furthermore, most *in vivo* studies concentrate on its effects with upstream proteins but lack research focused on Drebrin's impact on cognitive behavior in AD.<sup>19,23,24</sup> In this study, to explore the regularity of age, meticulous behavioral tests were conducted in APP/PS1 mice aged 4-16 months. A correlation analysis between Drebrin levels and behavioral data was performed. We found that Drebrin levels correlate with cognitive performance in Morris water maze (MWM), open field, and novel object tests. The results suggest that the expression and function of Drebrin may play an important role in the pathological process of AD. To verify this hypothesis, rAAV-Dbn1 vectors were injected into the hippocampus of AD mice to maintain a high level of Drebrin expression for months. Overall, this study examined the effects on the behavior and pathology in AD mice, providing further support for the treatment and research of this disease.

## 2 | MATERIALS AND METHODS

### 2.1 | Animals

APP<sup>swe</sup>/PS1 $\Delta$ E9 (APP/PS1) transgenic Alzheimer's disease model mice (C57BL/6J background) and wild-type C57BL/6J mice for

breeding were provided by the Institute of Experimental Animals of the Chinese Academy of Medical Science. All animals were maintained at 22-23°C on a 12-h light/dark cycle with *ad libitum* access to food and water. All animal experiments were approved by the Institutional Animal Care and Use Committee of the Institute of Laboratory Animal Science of Peking Union Medical College (ILAS-PL-2015-002). A total 12 female AD mice aged 4 months, 11 sex-matched AD mice aged 8 months and 10 per group sex-matched AD mice aged 12 or 16 months were tested using behavioral experimentation. More than 15 sex-matched AD mice were injected with rAAV-zsGreen-Dbn1 vector at 2 months of age, composing the APP/PS1-Dbn1 group, and sex- and age-matched AD mice were injected with rAAV-tdTomato vector to serve as the control group. In addition, we used 11 sex- and age-matched AD mice without any injection as the APP/PS1 group and 13 sex- and age-matched C57BL/6J mice under normal conditions as the WT group. The behaviors of all mice were examined after injection at 6 months. To investigate Drebrin expression level and pathological effect, Western blot, immunohistochemical staining, and immunofluorescence staining were performed with brain tissue.

### 2.2 | Behavioral tests

#### 2.2.1 | Morris water maze (MWM) test

The MWM test, which forces rodents to swim and trains them to search for a hidden platform under the water's surface,<sup>25</sup> was used to assess learning and memory capabilities of mice in our study. The apparatus was a white circular pool with a diameter of 100 cm and a height of 50 cm. The pool was imaginarily divided into four equal quadrants that were numbered 1, 2, 3, and 4. The first quadrant was the target quadrant with a cylindrical hidden platform (9 cm diameter, 27 cm height) in its center. The pool was filled with water at 23±1°C and was made opaque with nonfat milk powder. A flag, which the mice could use to navigate the maze, was positioned above the pool wall at a constant location during testing. A video camera tracked the swimming path of every mouse. All activities were analyzed by Ethovision XT (Noldus, Wageningen, the Netherlands) monitoring analysis software. The test included three phases, including visual platform, hidden platform to start, and probe tests. At the midpoint of the pool wall of the third quadrant, mice were placed in the water and swam with the cue flag. In this stage, mice could board the visual platform for no more than 60 seconds. Each mouse could be guided to board the platform and stand on the platform for 20 seconds. The second stage was conducted over five consecutive days. In this stage, the platform was submerged 1 cm under the water's surface and hidden by opaque milk. Each mouse was placed in the water from the pool wall in any quadrant except the platform quadrant. If mice explored in the pool and escaped onto the platform for 5 seconds within 60 seconds, the total time was recorded as the escape latency. If the mouse failed to board the platform within 60 seconds, it was guided to the platform by the experimenter and allowed to stand on it for 15 seconds. Each mouse was trained three times daily starting in a different quadrant each trial. Time intervals between every two quadrant training sessions were not

less than 30 minutes. Mice were wiped with a dry towel and dried by a heater after each session. All activities were recorded, including escape latency, success rate (ie, the rate of board on the platform on the fifth day), and swimming trace. The platform was removed on the sixth day, and mice were placed in the water from the middle of the pool wall of the third quadrant and allowed to swim freely for 60 seconds. All activities were recorded, including time spent in the target quadrant, frequency of crossing the target quadrant, swimming trace. All results were analyzed by Ethovision XT monitoring analysis software.

### 2.2.2 | Open field test

An open field test was used for tracking a variety of behavioral and emotional changes of animals in a novel open environment, such as probe behavior, autonomous activities, and anxiety.<sup>26</sup> The test apparatus was 50 cm in length, 50 cm wide, and 40 cm high. It was divided into border, center, and intermediate zones. Each mouse was placed in the same position of the field and tracked with a video camera for 5 minutes. All activities were analyzed by Ethovision XT monitoring analysis software. These activities included total distance, frequency in the center zone, moving speed, frequency of grooming, frequency of rearing, etc. The apparatus was cleaned with 75% alcohol between every two mice tested to eliminate odor.

### 2.2.3 | Novel object test

A novel object test was used to examine recognition ability because innate curiosity prompts rodents to explore novel objects. The apparatus was 50 cm in length, 50 cm wide, and 40 cm high in a quiet environment. The test included three stages: acclimation, familiarity, and test stages. The first and second day was the adaptation stage in which mice performed autonomous activities. The third and fourth day was the familiarity stage in which two toy bricks (2×2 cm) of the same shape, size, and color were placed in opposite corners. The fifth day was the test stage in which one of toy bricks was changed to a brick of a different shape and color. Each mouse was placed in the arena for 5 minutes during each stage. The probe time to a new object (TN) and familiar object (TF) was recorded with a video camera. The object probe was defined by the cumulative time of a mouse's nose in the sniffing zone, which was defined as a 2 cm radius around the object's rim. All behavioral results were recorded and analyzed by Ethovision XT monitoring analysis software. Recognition abilities were calculated by the Discrimination Index (DI) equation:  $DI = (TN + TF / TN + TF) \times 100\%$ .<sup>27</sup> The apparatus was cleaned with 75% alcohol between every two mice tested to eliminate odor.

### 2.2.4 | rAAV9-Dbn1 vector production and purification

Synthesis of mouse Dbn1 (NM\_001177371) fragments and production and purification of a viral vector were performed by Viraltherapy technologies (Wuhan, China). pAAV-IRES-ZsGreen containing two restriction enzyme cutting sites named BamHI and XhoI was the

plasmid vector. The mDbn1 fragments were connected to pAAV-IRES-ZsGreen plasmid vectors (pAAV-mDbn-IRES-ZsGreen). The plasmid vectors transformed competent cells and were extracted for sequence analysis. Sequence alignment showed consistency between the pAAV-mDbn-IRES-ZsGreen and design sequence. The recombinant plasmid infected 293 AAV cells, and then, rAAV9-Dbn1 vectors were produced and purified with a high titer of  $5 \times 10^{12}$  vg/mL. Finally, real-time Q-PCR was performed to assess expression efficiency of rAAV9-mDbn1 in HeLa recipient cells.

### 2.2.5 | Intrahippocampal injections

To perform accurate injections, we injected trypan blue diluent into the hippocampi of mice using a stereotaxic apparatus, which served as a preliminary experiment. The injection coordinates were determined according to *The Mouse Brain in stereotaxic coordinates*<sup>28</sup> written by George Paxinos and Keith B.J. Franklin as follows: bregma, -2.1 mm; sagittal suture,  $\pm 1.35$  mm; depth, 1.75 mm. We injected 2  $\mu$ L of 0.4% trypan blue diluent dissolved in PBS into the hippocampus of mice bilaterally with a 10- $\mu$ L capacity microinjector. Subsequently, we injected 2  $\mu$ L of rAAV-zsGreen-Dbn1 or rAAV-tdTomato vector with a titer of  $5 \times 10^{12}$  vg/mL at the same injection coordinates into the mouse hippocampus bilaterally in the formal experiment. Approximately a month after injection, brains were extracted and cut into 10- $\mu$ m frozen coronal sections. Green (excitation wavelength of 493 nm) or red (excitation wavelength of 554 nm) fluorescence was observed with a Fluorescence Inversion Microscope System (Olympus, Tokyo, Japan) of the injection area. A fluorescent signal implied that the labeled gene was expressed and the injection placement was accurate. The remainder of the mice were reared for additional experiments.

### 2.2.6 | Western blot

Hippocampal tissue was solubilized in RIPA buffer with protease and phosphatase inhibitor (1:100, CST). Tissue lysates were centrifuged for 30 minutes at 17 320 g, and supernatants were harvested. Protein concentrations were determined by BCA kit (Beyotime, Shanghai, China). Equal amounts of protein (40  $\mu$ g) were dissolved in an SDS-PAGE buffer and separated by SDS-polyacrylamide gel electrophoresis. Next, proteins were transferred onto polyvinylidene difluoride membranes (0.45  $\mu$ m; Millipore, USA) and blocked for 1 hour with 5% nonfat dry milk in TBST (Tris buffer saline containing 0.1% Tween-20). Membranes were then incubated with a primary antibody (anti-Drebrin, 1:1000, Millipore) overnight at 4°C. The next day, membranes were washed with TBST and incubated with a secondary antibody (ZSGB-BIO). Proteins were revealed with an automatic chemiluminescence imaging analysis system (Tanon 5500; Tanon Science & Technology).

### 2.2.7 | Immunohistochemical staining

Brains were fixed with 10% formalin solution for 48–72 hours. Brains were then dehydrated, embedded in paraffin, and cut into 4- $\mu$ m coronal sections. To label with a corresponding antibody, three hippocampal

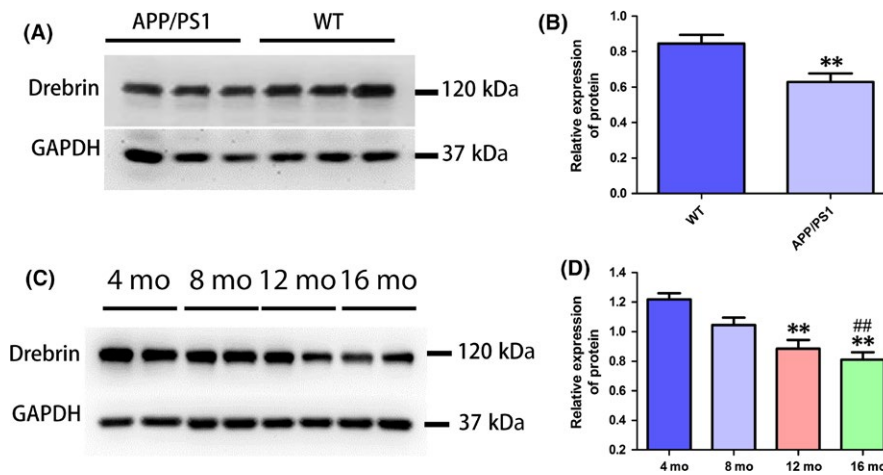


**FIGURE 1** Expression level of Drebrin protein in mouse hippocampal tissue. (A,B) Western blot analysis for Drebrin protein expression levels in 12-month-old APP/PS1 mouse hippocampus and that of age-matched WT mice. Relative protein expression levels adjusted by GAPDH ( $n=9$  per group, Student's *t* test,  $**P<.01$ ; APP/PS1 mice vs age-matched WT mice). (C,D) Western blot analysis for Drebrin protein expression levels in 4-, 8-, 12-, and 16-month-old APP/PS1 mouse hippocampi. Relative protein expression levels adjusted by GAPDH ( $n=6$  per group, Tukey's test,  $**P<.01$ , 4-month APP/PS1 vs 16-month APP/PS1;  $**P<.01$ , 4-month APP/PS1 vs 12-month APP/PS1;  $##P<.01$ , 8-month APP/PS1 vs 16-month APP/PS1)

slices from the same anatomical regions of each mouse were processed. Paraffin sections were dewaxed and rehydrated by gradient alcohol baths. Sections underwent antigen retrieval in a sodium citrate buffer bath and blocked with normal goat serum sealing fluid (ZSGB-BIO). The tissue was then incubated with an anti-Drebrin antibody (1:1000, Millipore) or anti- $A\beta$ 17-24 antibody (1:300, 4G8, BioLegend) overnight at 4°C. HRP-labeled anti-rabbit/mouse IgG (ZSGB-BIO) was used to identify the antigen, and a DAB (ZSGB-BIO) reaction was performed to visualize the stain. Sections were imaged by Olympus cellSens (Japan) software and analyzed by Image J (NIH) software (Media Cybernetics Inc., Rockville, MD, USA).

### 2.2.8 | Immunofluorescence staining

We selected three hippocampal slices from the same anatomical regions of each mouse using each antibody for staining. Paraffin sections were dewaxed and hydrated by gradient alcohol baths. Sections underwent antigen retrieval with a sodium citrate buffer bath and blocked with normal goat serum sealing fluid (ZSGB-BIO). The sections were then incubated with anti-GFAP antibody (1:500, abcam), anti-F-actin antibody (1:500, sigma), anti-NMDAR1 antibody (1:500, abcam), anti-MAP-2 antibody (1:300, abcam), or anti-Syn1 antibody (1:300, abcam). After washed with a PBS buffer (0.01 mol/L), the sections were incubated with FITC/TRITC labeled anti-rabbit/mouse IgG and counterstained with DAPI (ZSGB-BIO). Sections were imaged by FV10-ASW4.1.2.1 (Olympus) software and analyzed by ImageJ (NIH) software.

### 2.3 | Statistical analysis

Statistical analyses were performed by using SPSS 13.0 for windows (SPSS Inc., Chicago, IL). The results are expressed as the means $\pm$ SEM. Student's *t* test was used for two-group analysis. Tukey's test was used for multiple group analysis. The Pearson correlation test was used for correlation analysis. A *P* value  $<.05$  was considered statistically significant.

## 3 | RESULTS

### 3.1 | The expression of Drebrin is downregulated in the hippocampus of aged AD mice compared with that of age-matched WT and young adult AD mice

To observe the regularity of Drebrin expression in APP/PS1 mouse hippocampal tissue, we measured Drebrin expression levels using Western blot in 12-month-old APP/PS1 AD mice and age-matched WT hippocampi (Figure 1A,B). The levels of Drebrin in APP/PS1 mice were significantly lower than in the WT group ( $n=9$  per group,  $P<.01$ ). The data were consistent with the low level of Drebrin measured in AD patient hippocampi compared with age-matched subjects in the human literature.<sup>19</sup> These results imply that Drebrin may be involved in the degeneration of the central nervous system. To confirm the correlation between the expression levels of Drebrin and aging, we detected the expression of the Drebrin protein in the hippocampus of adult APP/PS1 mice at different ages (4, 8, 12, and 16 months). Drebrin levels in the 16-month group were significantly lower than those in the 4- and 8-month groups ( $P<.01$ ). Furthermore, Drebrin levels in the 12-month group were significantly lower than those in the 4-month group ( $P<.01$ ), and the levels in the 8-month group were significantly lower than those in the 4-month group ( $P<.05$ ) (Figure 1 C,D). These results indicate that the expression of Drebrin in the hippocampus of AD mice decreases with age.

### 3.2 | Cognitive ability of APP/PS1 mice decreases with age

The MWM is a classic experiment to test the ability of learning and memory in mice by testing their navigation ability to find a hidden platform with respect to landmark cues. In the navigation stage, the escape latency of mice in all groups was shortened with more days of training. The escape latency of AD mice is also generally longer

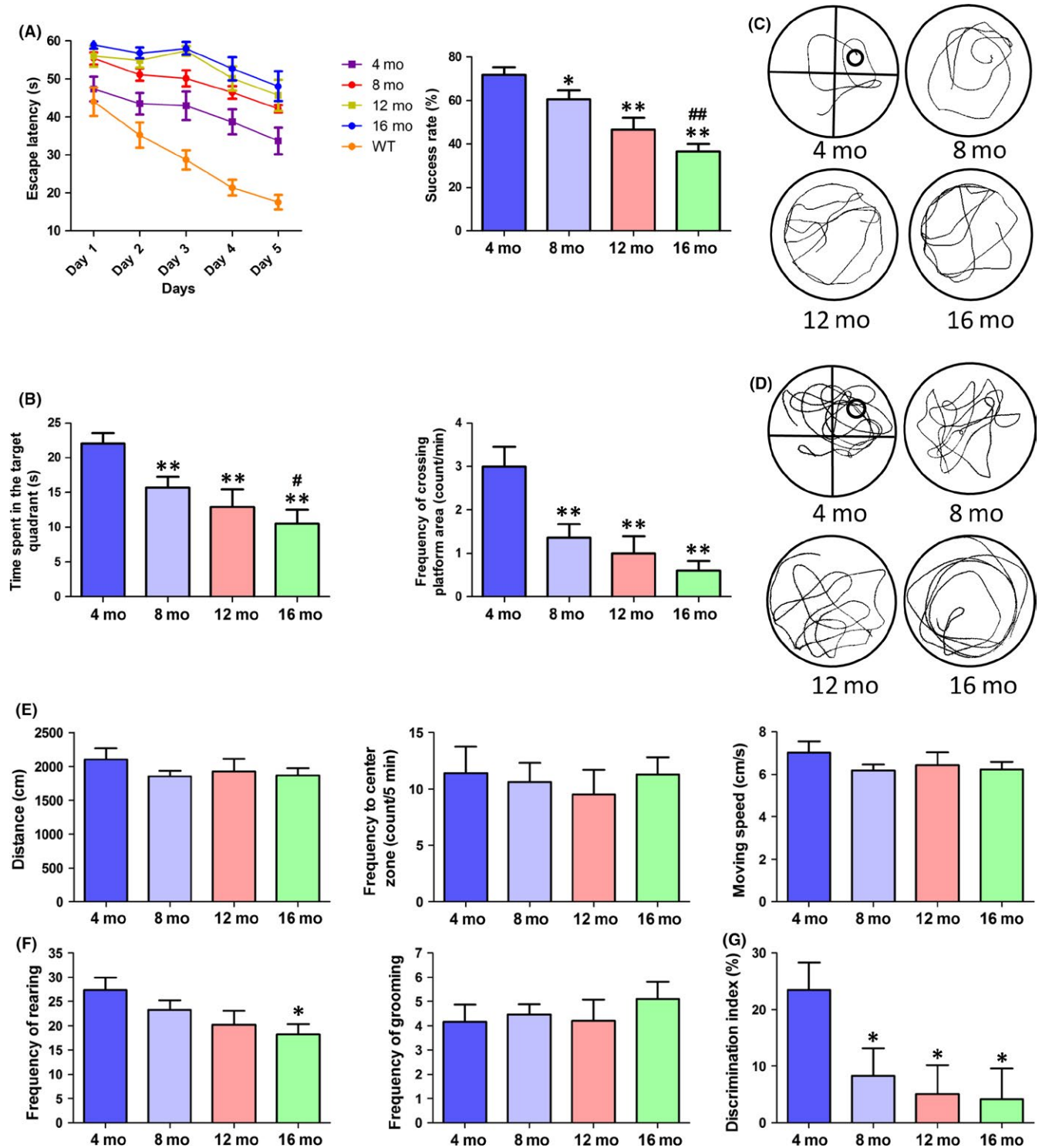
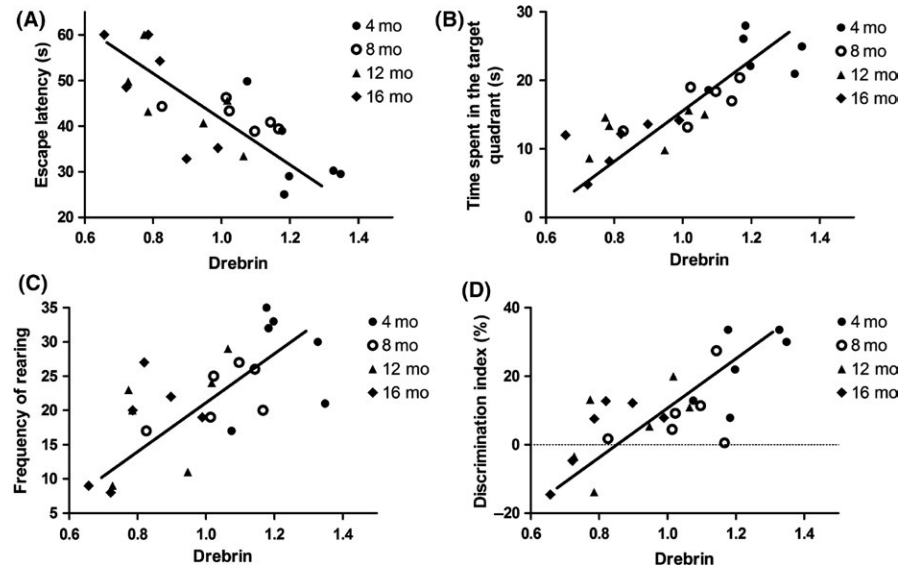


**FIGURE 2** Behavioral performance of APP/PS1 mice in different months (4, 8, 12, and 16 mo). (A) The escape latency during 5 days of testing and the success rate of locating the platform on the last day of the MWM test ( $n=13$  for WT,  $n=13$  for 4-mo-old APP/PS1 mice,  $n=11$  for 8-mo-old APP/PS1 mice,  $n=10$  for 12- or 16-mo-old APP/PS1 mice, two-way repeated-measures ANOVA, Tukey's test,  $*P<.05$ ,  $**P<.01$ , 4-mo-old APP/PS1 vs WT mice;  $\#P<.05$ ,  $\#\#P<.01$ , 4- vs 16-mo-old mice;  $*P<.05$ ,  $**P<.01$ , vs 4-mo-old mice,  $\#\#\#P<.01$ , vs 8-mo-old). (B) Time spent in the target quadrant and frequency of crossing the target quadrant during the probe test in the MWM test (one-way ANOVA, Tukey's test,  $*P<.05$ ,  $**P<.01$ , vs 4-mo-old mice;  $\#P<.05$ ,  $\#\#P<.01$ , vs 8-mo-old mice). (C) The track of locating swim. (D) The track of probe test. (E) Total distance, frequency to the center zone and moving speed in the open field test. (F) Frequency of rearing and grooming in the open field test ( $n=12$  for 4-mo-old,  $n=11$  for 8-mo-old, and  $n=10$  for 12- or 16-mo-old APP/PS1 mice, one-way ANOVA, Tukey's test,  $*P<.05$ , 16 mo vs 4 mo APP/PS1). (G) Discrimination index in the new object test (one-way ANOVA, Tukey's test,  $*P<.05$ , vs 4-mo-old APP/PS1 mice)

**FIGURE 3** Correlations of hippocampal Drebrin expression with behavioral performance in AD mice at ages 4, 8, 12, and 16 mo (A) Correlation of Drebrin expression level with escape latency ( $r = -.770$ ,  $P < .001$ , Pearson correlation test). (B) Correlation of Drebrin expression level with time spent in the target quadrant ( $r = .842$ ,  $P < .001$ , Pearson correlation test). (C) Correlation of Drebrin expression level with frequency of rearing ( $r = .658$ ,  $P < .001$ , Pearson correlation test). (D) Correlation of Drebrin expression level with DI ( $r = .757$ ,  $P < .001$ , Pearson correlation test)



than that of WT mice, especially during training sessions of the third, fourth, and fifth days. The escape latency of 4-month-old AD mice was significantly longer than that of WT mice ( $P < .01$ ). Furthermore, 16-month-old AD mice spent significantly longer to find the platform than 4-month-old AD mice ( $P < .01$ ). The data show that the escape latency in adult AD mice generally increases with age and significantly increased after 8 months. On the last day of training, the success rate of finding the platform also reflected age-related decline: 8-month-old mice were significantly slower than 4-month-old AD mice ( $P < .05$ ), 12- and 16-month-old mice were significantly slower than 4-month-old AD mice ( $P < .01$ ), and 16-month-old mice were significantly slower than 8-month-old AD mice ( $P < .01$ ). There was no significant difference between 16- and 12-month-old AD mice ( $P > .05$ ; Figure 2 A). In the probe test, the time spent in the target quadrant and the frequency of crossing the platform area of AD mice also showed a decreasing trend with age. The 8-, 12-, and 16-month-old AD mice spent significantly less time crossing the platform than the 4-month-old AD mice ( $P < .01$ ), and 16-month-old mice spent significantly less time than 8-month-old mice ( $P < .05$ ; Figure 2 B). All results showed that the learning, memory, and spatial localization ability of adult AD mice decreased with age. Subsequently, open field and novel object tests were conducted for further study. In the open field test, there was no significant difference in total distance, frequency to the center zone, and frequency of grooming (Figure 2E,F). However, the frequency of rearing tends to decrease with age (Figure 2F), especially in 16-month-old compared to 4-month-old AD mice ( $P < .05$ ). In the novel object test, the discrimination index (DI) percentage in 8-, 12-, and 16-month-old AD mice was significantly lower than in 4-month-old mice ( $P < .05$ ; Figure 2G).

### 3.3 | Drebrin protein expression in the hippocampus correlates with behavioral performance in different aged AD mice

To explore whether there was a correlation between the expression level of Drebrin and behavioral performance of AD mice of different

ages, a correlation analysis between behavioral data and corresponding Drebrin expression data in the same mouse was performed. The escape latency during the fifth day and the time spent in the target quadrant in MWM were detected in the analysis. The results show that there was a high correlation between Drebrin expression and escape latency ( $r = -.770$ ,  $P < .001$ ; Figure 3A) and time spent in the target quadrant ( $r = .842$ ,  $P < .001$ ; Figure 3B). These results suggest that decreased Drebrin expression may impact the memory and spatial localization ability of AD mice. The frequency of rearing in the open field test was assessed in the correlation analysis to detect whether Drebrin expression influences autonomic activities of AD mice. The data show a moderate correlation between Drebrin and the frequency of rearing ( $r = .658$ ,  $P < .001$ ; Figure 3C), indicating that Drebrin has no significant impact on autonomic activities in AD mice. The DI in the novel object test was compared with Drebrin, showing a significant correlation with Drebrin protein levels ( $r = .757$ ,  $P < .001$ ) (Figure 3D). This suggests that decreased Drebrin expression may impact memory ability and curiosity.

### 3.4 | Production of AAV9-mDbn1 vectors and expression in the hippocampus of AD mice

To further study the role of Drebrin in the central nervous system of AD mice, AAV9-mDbn1 was produced by the connection between a plasmid vector and a target fragment of Dbn1. The sequencing comparison confirmed Dbn1, including restriction site BamHI+XhoI and Kozak sequences, was highly consistent with the design sequence (Figure 4A, B). The expression efficiency of the AAV9-mDbn1 vector in HeLa cells was detected by Q-PCR, showing more effective expression than blank controls (Figure 4C,D,  $P < .01$ ). A 0.4% trypan blue diluent was injected into the hippocampi of mice using a stereotaxic apparatus to perform accurate injections (Figure 4E). Trypan blue was injected smoothly into the targeted position. Dissection revealed that there was no trypan blue infiltration at the bregma, areas surrounding the hippocampus, occipital area, or in the 3rd ventricle. Subsequently,

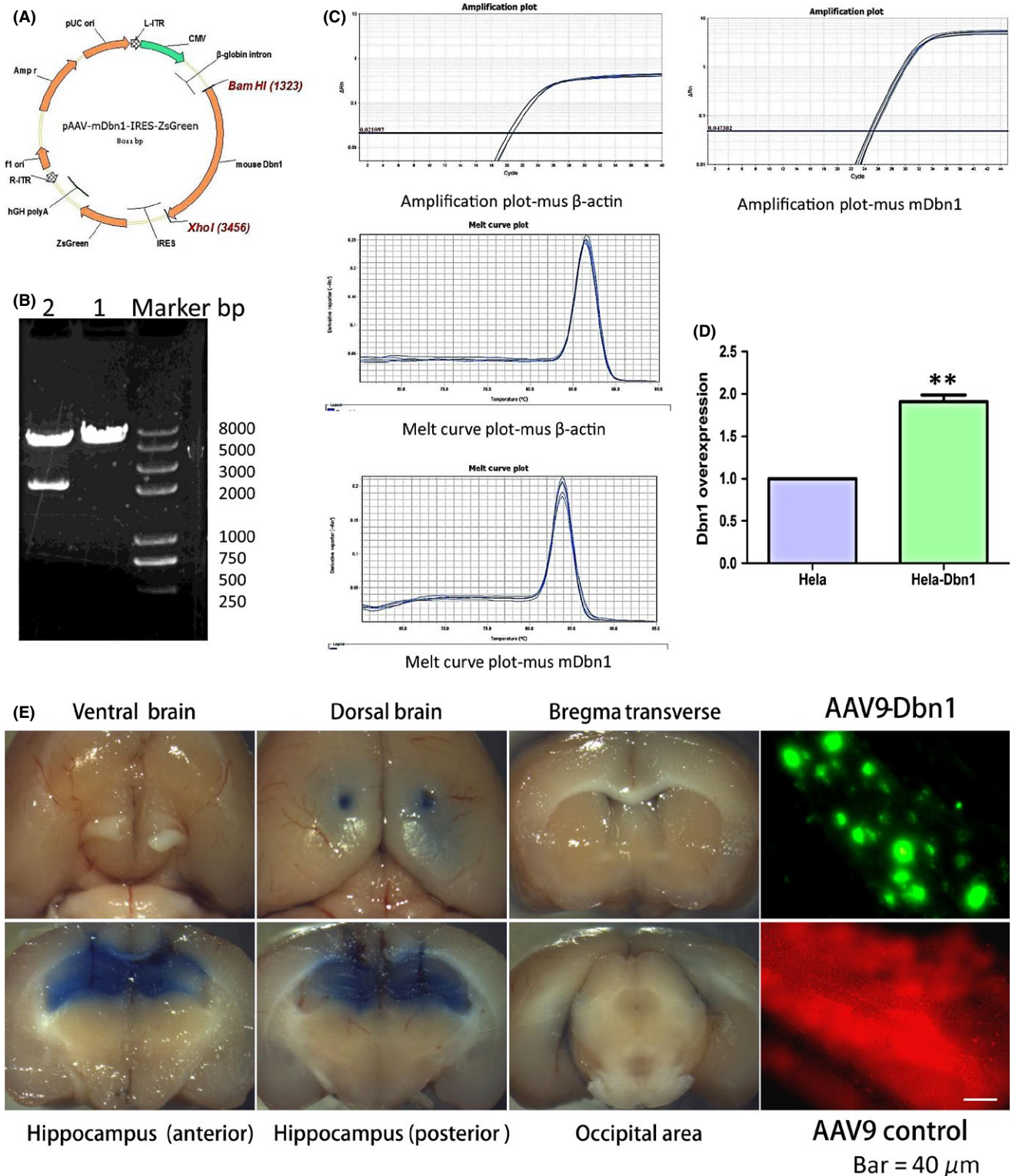


**FIGURE 4** Structure of pAAV-mDbn1-IRES-ZsGreen, expression efficiency of Dbn1, mouse hippocampal injection, and high expression of Drebrin protein in mouse hippocampus. (A,B) Basic structure of pAAV-mDbn1 plasmid and enzyme identification. (C,D) Expression efficiency of mDbn1 was detected by Q-PCR. (E) Mouse hippocampi were injected with trypan blue; AAV9-Dbn1 (excitation wavelength of 493 nm) showing green fluorescence or AAV9 vector (excitation wavelength of 554 nm) showing red fluorescence in the mouse hippocampus (Scale bar=40  $\mu$ m). (F) The Drebrin protein was detected by immunohistochemical staining in the APP/PS1-Dbn1 group and control AD group (n=8 per group, Student's t test, \* $P$ <.05, \*\* $P$ <.01, APP/PS1 vs control; Scale bar=40  $\mu$ m)

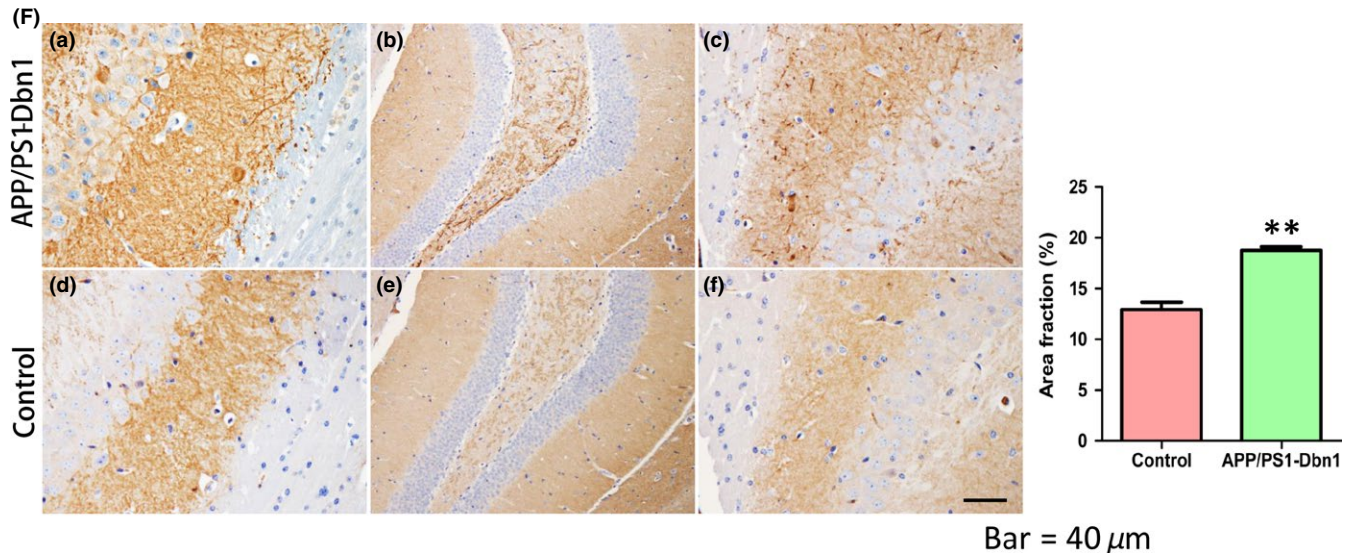


**FIGURE 4** (Continued)

AAV9-mDbn1 vectors with a green fluorescence label or AAV9 vectors with a red fluorescence label were injected into hippocampi of AD mice. A month after injection, green or red fluorescence was observed by a Fluorescence Inversion Microscope System in the hippocampus (Figure 4E). A fluorescent signal implies that the labeled gene is expressed and the injection coordinates are accurate.

### 3.5 | Cognitive ability improved significantly in APP/PS1-Dbn1 mice

The escape latency of mice in all groups was shortened with increased days of training in the navigation stage of MWM. An escape latency scatter plot shows that there are no significant differences between the control and APP/PS1 groups, but the APP/PS1-Dbn1 group did spend less time than the two groups ( $P < .05$ ). On the last day of training, the success rate of finding the platform showed that the control group mice were significantly slower than the APP/PS1-Dbn1 mice ( $P < .05$ ; Figure 5A). In the probe test, the time spent in the target quadrant and the frequency of crossing the platform area in all groups of mice also showed different performances. APP/PS1-Dbn1 mice spent significantly more time in the target quadrant and had a significantly greater frequency of crossing the platform area than the control group mice ( $P < .05$ ; Figure 5B). The data show that the learning, memory, and spatial localization ability of APP/PS1-Dbn1 mice improved significantly. The open field and novel object tests were performed for further study. There were no significant differences in total distance, frequency to the center zone, and frequency of grooming between groups in the open field test (Figure 5E,F). Nevertheless, the frequency of rearing in APP/PS1-Dbn1 mice was significantly higher than in the control group ( $P < .05$ ) and there was no significant difference in WT mice ( $P > .05$ ; Figure 5F). In the novel object test, the DI in APP/PS1-Dbn1 mice was significantly higher than in control and APP/PS1 mice ( $P < .05$ ; Figure 5G). All results suggest that AAV9-Dbn1 vectors in the hippocampus can promote better performance in AD mice

than non-Dbn1 AD mice in MWM, open field, and novel object tests. The improved behavioral performance of APP/PS1-Dbn1 mice may be due to high levels of the Drebrin protein.

### 3.6 | The expression level of Drebrin in APP/PS1-Dbn1 mouse hippocampus was significantly increased; the pathological lesion of AD was alleviated in APP/PS1-Dbn1 mice

In this study, the expression of Drebrin in the hippocampus of APP/PS1-Dbn1 and control mice was detected by immunohistochemistry to verify the hypothesis that positive behavioral performance of APP/PS1-Dbn1 mice may be due to high levels of the Drebrin protein. The positive area fraction showed that APP/PS1-Dbn1 mice had significantly more staining than the control group ( $P < .01$ ; Figure 4F). The result suggests a high expression level of Drebrin can improve behavioral activities in AD mice. The  $A\beta$  plaques derived from deposited the  $A\beta$  peptide are a typical pathology characteristic of AD, which increases with age and is aggravated in AD patients.<sup>29</sup> Similarly, the same lesions and features also exist in the brains of APP/PS1 mice.<sup>30</sup> The anti- $A\beta$ 17-24 antibody was used to detect  $A\beta$  plaques in immunohistochemical staining in mice across all groups to further detect the relationship between high levels of the Drebrin protein and the deposited  $A\beta$  peptide. The results show that the area fraction and number of plaques in the hippocampus of APP/PS1-Dbn1 mice are markedly reduced ( $P < .01$ ; Figure 6A,B). Astrocytes, which can secrete a variety of inflammatory factors and mediate signal transduction, are widely distributed in the brain.<sup>31</sup> Astrocyte reactivity increases or is accompanied by morphological changes when cerebral injury occurs.<sup>32,33</sup> GFAP, a specific marker to detect astrocytes, was applied to investigate postinjection changes of hippocampal astrocytes by immunofluorescent staining in mice. The results showed that the APP/PS1-Dbn1 group had significantly fewer astrocytes than the control group ( $P < .01$ ; Figure 6C,F). Furthermore, the control group



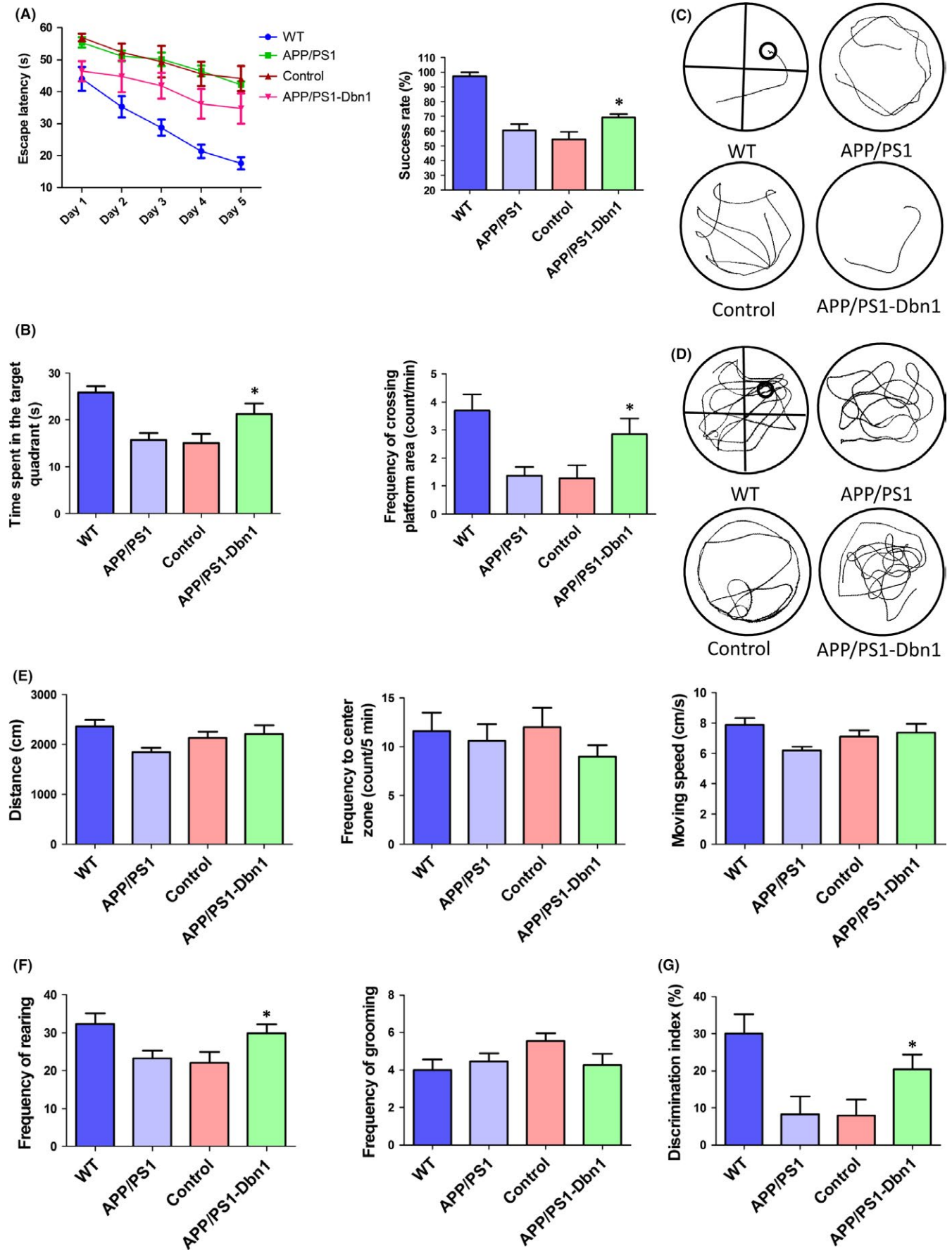


**FIGURE 5** The behavioral performance of mice in different groups (WT, APP/PS1, control, and APP/PS1-Dbn1). (A) The escape latency during 5 days and the success rate of locating the platform on the last day of the MWM test (n=13 for WT, n=11 for APP/PS1, n=11 for control, n=13 for APP/PS1-Dbn1, two-way repeated-measures ANOVA, Tukey's test, \* $P < .05$ , control vs APP/PS1-Dbn1). (B) Time spent in the target quadrant and frequency of crossing the target quadrant during the probe test in the MWM test (one-way ANOVA, Tukey's test, \* $P < .05$ , control vs APP/PS1-Dbn1). (C) The track of locating swim. (D) The track of probe test. (E) Total distance, frequency to the center zone and moving speed in the open field test. (F) Frequency of rearing and frequency of grooming in the open field test (n=13 for WT, n=11 for APP/PS1, n=11 for control, n=11 for APP/PS1-Dbn1, one-way ANOVA, Tukey's test, \* $P < .05$ , control vs APP/PS1-Dbn1). (G) Discrimination index in the new object test (n=12 for WT, n=11 for APP/PS1, n=11 for control, n=11 for APP/PS1-Dbn1; one-way ANOVA, Tukey's test, \* $P < .05$ , control vs APP/PS1-Dbn1)

had significantly more astrocytes than the other three groups. These findings suggest that operative injury activates astrocytes, but high levels of Drebrin may inhibit over activated astrocytes.

### 3.7 | Relative protein changes of Drebrin in APP/PS1-Dbn1 mice

The immunofluorescence assays to detect F-actin, NMDAR1, MAP-2, and Syn1 were performed to investigate the impact of increased Drebrin in AD mice. Studies have reported F-actin combines with Drebrin to maintain LTP and accompany the reduction of Drebrin.<sup>34</sup> But whether increased Drebrin can impact F-actin has not yet been reported. Furthermore, overactivated NMDAR can accelerate Drebrin degradation,<sup>29</sup> but whether Drebrin can impact NMDAR needs to be studied further. Microtubule-associated protein MAP-2, which is involved in the formation of neuronal cytoskeleton, is an important marker of neuronal microtubules, which is decreased in AD brains.<sup>35</sup> Synaptic-associated protein Syn1 is reduced in AD brains and plays a pivotal role in synapse formation, vesicle trafficking, neurotransmitter release, etc.<sup>36</sup> The results showed that F-actin in APP/PS1-Dbn1 mice was notably higher than in control and APP/PS1 mice ( $P < .01$ ; Figure 6D,F), and MAP-2 in APP/PS1-Dbn1 mice had significantly more staining than control mice ( $P < .01$ ; Figure 7A,C). These findings suggest that effective expression of Drebrin plays a positive role in aggregating neuronal microtubules in AD mice. However, there were no significant differences between groups for NMDAR1 and Syn1 ( $P > .05$ ; Figure 6E,F; Figure 7B,C). These findings suggest Drebrin cannot regulate the expression of NMDAR1 and Syn1 in a positive manner.

## 4 | DISCUSSION

In this study, the results suggest that effective expression of the Drebrin protein in the hippocampus of AD mice via injection of rAAV9-Dbn1 vectors can improve cognitive competence and alleviate lesions of AD. Previous studies report that Drebrin plays a key role in maintaining long-term memory<sup>37</sup>; moreover, it also display its function in cell migration, synaptic development, and plasticity.<sup>19,20</sup> Synaptic remodeling is a form of rapid upregulative nervous transmission under repeated axonal stimulation, which is the basis of memory by cytomorphosis.<sup>38,39</sup> Neurodegenerative diseases, such as AD, have been found to manifest cognitive impairment

symptoms that are related to the synaptic damage.<sup>30,40,41</sup> In addition, postmortem reports find that Drebrin in AD patients is notably lower than in healthy control brains in the hippocampus and cortex.<sup>19</sup> Aged AD mice were also found to have marked declined of Drebrin<sup>42</sup> that was also confirmed in this study. We therefore hypothesize that the expression level of Drebrin in AD mice may correlate with their behavioral activities, especially cognitive behavior. In our study, the expression level of Drebrin in 4- to 16-month-old AD mice was detected by Western blotting. We found that the Drebrin protein decreased with age. Subsequently, the MWM, open field and novel object tests were performed in 4- to 16-month-old AD mice. The MWM was used to assess learning and memory capabilities of rodents.<sup>43</sup> The open field test was used to investigate autonomous activities and to probe behavior. Finally, the novel object test was conducted to detect recognition ability to novel objects.<sup>44,45</sup> We found a significant difference in all three tests, especially in MWM and novel object tests. These data show a significant decline in cognitive and autonomous activities with age. The correlation analysis data showed that the expression level of Drebrin was significantly correlated with behavioral performance in different ages of adult AD mice. Based on these results, we suggest that Drebrin serves an important role in the central nervous system of AD mice, and injecting the rAAV9-Dbn1 vector into the hippocampus of 2-month-old AD mice maintains an effective expression of Drebrin for months.

Approximately 6 months later, we found APP/PS1-Dbn1 mice performed better than control and APP/PS1 mice. This was evident in all of the behavioral tests, especially in MWM and novel object tests. Although most previous research has been conducted on the role of Drebrin in neuronal development and long-term memory,<sup>46</sup> there are few reports on the overexpression of Drebrin in an AD model in vivo, especially during behavioral tests. In this study, we observed the behavior of mice in detail and further provide evidence for the effect of Drebrin on the central nervous system and provide primary experimental resources for gene therapy. To confirm that Drebrin can impact pathological changes of AD at the molecular level, we performed immunohistochemical staining to detect related proteins. Accumulative  $A\beta$  in AD activates glial cells and produces various inflammatory factors to aggravate neurotoxicity, which contributes to synaptic depression and cognitive impairment.<sup>47-49</sup> We found that the area fraction and number of plaques of  $A\beta$  in the hippocampus of APP/PS1-Dbn1 mice are significantly reduced. Cell research showed that the  $A\beta_{42}$  oligomer can reduce Drebrin in hippocampal neurons

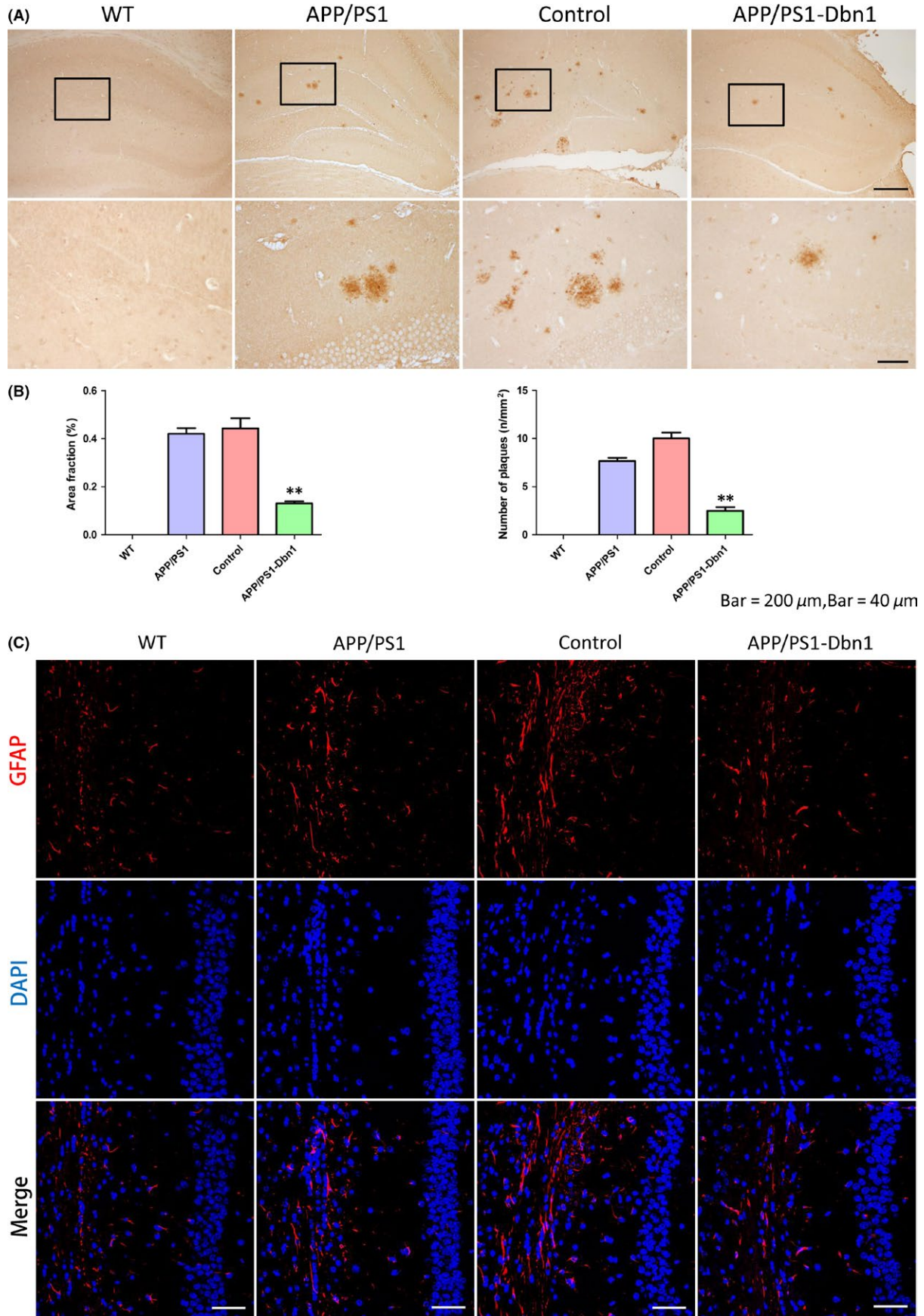


**FIGURE 6** (Continued)

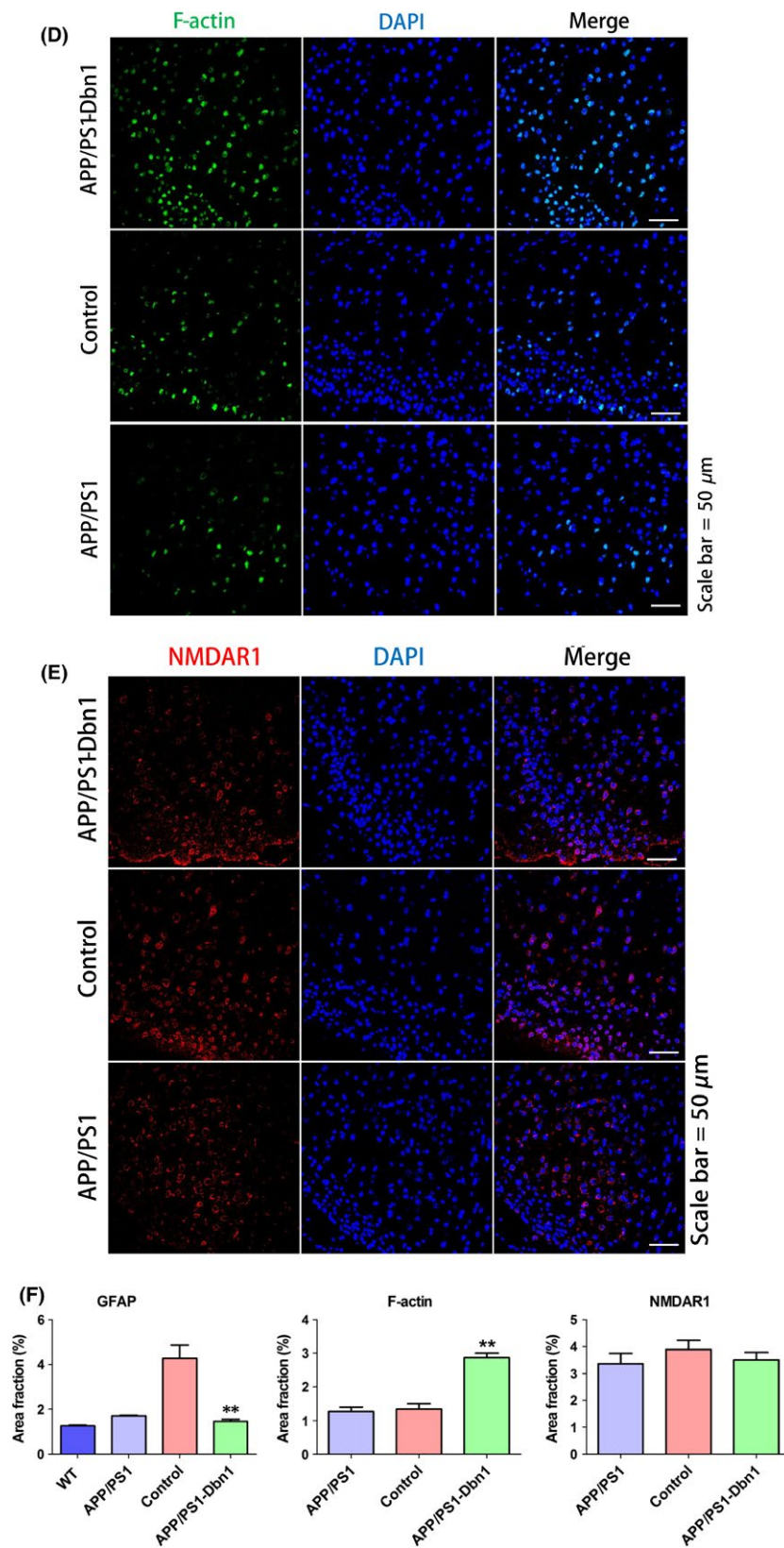


**FIGURE 6** Relative protein expression of Drebrin and pathological changes in different groups. (A, B) Immunohistochemical staining shows amyloid protein expression in the hippocampus of different groups (Scale bar=200  $\mu$ m, Scale bar=40  $\mu$ m). (C) Immunofluorescence staining shows GFAP expression in each group. (D) Immunofluorescence staining shows F-actin expression in each group. (E) Immunofluorescence staining shows NMDAR1 expression in each group. (F) Area fraction of GFAP, F-actin and NMDAR1 (Scale bar=50  $\mu$ m, n=6 per group, one-way ANOVA, Tukey's test, \* $P$ <.05, \*\* $P$ <.01, control vs APP/PS1-Dbn1)

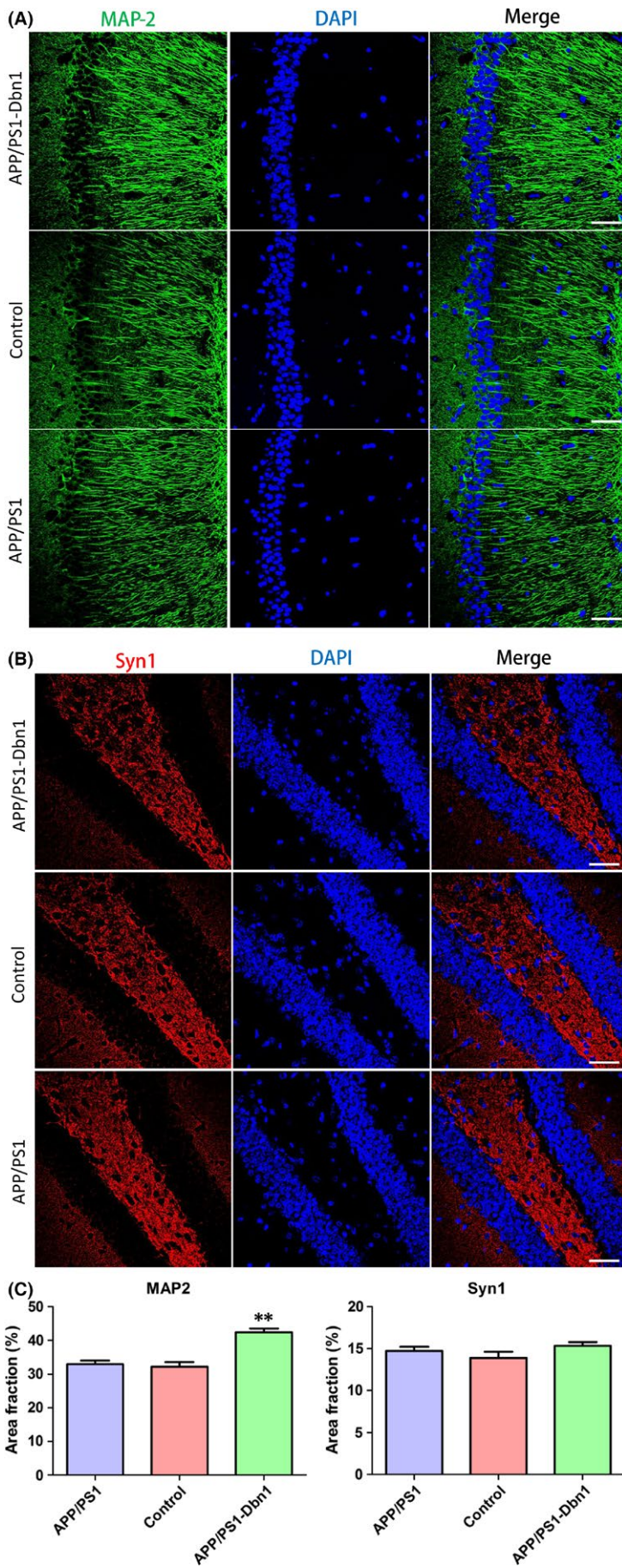


**FIGURE 7** Relative protein expression in different groups of mice brain. (A) Immunofluorescence staining shows MAP-2 expression in each group. (B) Immunofluorescence staining shows Syn1 expression in each group. (C) Area fraction of MAP-2 and Syn1 (n=6 per group, one-way ANOVA, Tukey's test, \* $P < .05$ , \*\* $P < .01$ , control vs APP/PS1-Dbn1)

of mice,<sup>50</sup> but there are rarely reports on the impact of Drebrin on  $A\beta$ . We suggest that Drebrin may play a role in inhibiting  $A\beta$  generation or accelerating its degradation. Astrocytes, distributed widely in the brain to maintain homeostasis, provide nutrition, regulates energy metabolism, and transduces signals, among other duties.<sup>51</sup> However, astrocyte reactivity increases and reactive gliosis are main factors of neuroplasticity and CNS regeneration when cerebral injury occurs.<sup>52</sup> Activated astrocytes can increase  $A\beta$  by secreting inflammatory factors and complements.<sup>53,54</sup> GFAP is a specific marker of astrocytes, which modulates the morphology and quantity of astrocytes to be used to evaluate cerebral status. We found that GFAP in an injection area increased the quantity and changed the morphology in the control group, implying that astrocytes were activated by injection and vector stimulation. Conversely, there are rarely activated astrocytes in the APP/PS1-Dbn1 group, in which the quantity was close to the APP/PS1 group. These results suggest that effective expression of Drebrin may inhibit the activation of astrocytes.

Drebrin regulates memory by binding or depolymerization with F-actin, which interacts with neural microtubules mediated by Drebrin.<sup>55</sup> In addition, the distribution of F-actin was also adjusted by Drebrin.<sup>56</sup> We found that increased levels of Drebrin can promote an increase in the quantity of F-actin. MAP-2 is distributed in the neuronal cytoplasm, especially in dendrites. It can adjust microtubule assembly and stabilize the cytoskeleton to maintain neuron dendritic growth.<sup>57-59</sup> In this study, MAP-2 in the APP/PS1-Dbn1 group was significantly higher than in the control group in the hippocampus. We suggest that increased levels of Drebrin can stabilize neuronal dendrites to improve cognitive function. Thus, rAAV9-mediated effective expression of Drebrin in the hippocampus of AD model mice may provide a valid method to improve cognitive ability by inhibiting  $A\beta$ .

## 5 | CONCLUSION

Our study showed that hippocampal Drebrin protein expression levels in adult APP/PS1 mice decline with age. Furthermore, our behavioral data demonstrated that cognitive and probe activities decline with age. A correlation analysis showed that the expression level of the Drebrin protein significantly correlates with behavioral performance in AD mice. rAAV9-Dbn1 vectors can maintain an effective expression level of Drebrin, which improves performance and alleviates lesions in AD mice. These results may provide some valid resources for therapy and research of AD.

## ACKNOWLEDGMENTS

This work was funded by CAMS Innovation Fund for Medical Sciences (CIFMS): Chuan Qin major collaborative innovation project, China (2016-12M-2-006).

## CONFLICT OF INTEREST

The authors declare no conflict of interest.

## REFERENCES

- Dubois B, Feldman HH, Jacova C, et al. Revising the definition of Alzheimer's disease: a new lexicon. *Lancet Neurol.* 2010;9:1118-1127.
- De Felice FG. Alzheimer's disease and insulin resistance: translating basic science into clinical applications. *J Clin Invest.* 2013;123:531-539.
- Liu S, Cai W, Pujol S, Kikinis R, Feng DD, The Alzheimer's Disease Neuroimaging Initiative. Cross-view neuroimage pattern analysis in Alzheimer's disease staging. *Front Aging Neurosci.* 2016;8:23.
- Prince M, Wimo A, Guerchet M, Ali GC, Wu YT, Prina M. World Alzheimer Report 2015: The Global Impact of Dementia. 2015
- Alzheimer's Association. 2016 Alzheimer's disease facts and figures. *Alzheimers Dement.* 2016;12:459-509.
- Bertram L, Tanzi RE. The genetics of Alzheimer's disease. *Prog Mol Biol Transl Sci.* 2012;107:79-100.
- Hyman BT, Phelps CH, Beach TG, et al. National Institute on Aging-Alzheimer's Association guidelines for the neuropathologic assessment of Alzheimer's disease. *Alzheimers Dement.* 2012;8:1-13.
- Li Y, Sun H, Chen Z, Huaxi X, Bu G, Zheng H. Implications of GABAergic neurotransmission in Alzheimer's disease. *Front Aging Neurosci.* 2016;8:31.
- Jack CR Jr, Knopman DS, Jagust WJ, et al. Hypothetical model of dynamic biomarkers of the Alzheimer's pathological cascade. *Lancet Neurol.* 2010;9:119-128.
- Giese KP, Aziz W, Kraev I, Stewart MG. Generation of multi-innervated dendritic spines as a novel mechanism of long-term memory formation. *Neurobiol Learn Mem.* 2015;124:48-51.
- Jung G, Kim EJ, Cicvaric A, et al. Drebrin depletion alters neurotransmitter receptor levels in protein complexes, dendritic spine morphogenesis and memory-related synaptic plasticity in the mouse hippocampus. *J Neurochem.* 2015;134:327-339.
- Crews L, Masliah E. Molecular mechanisms of neurodegeneration in Alzheimer's disease. *Hum Mol Genet.* 2010;19:R12-R20.
- Sclip A, Tozzi A, Abaza A, et al. c-Jun N-terminal kinase has a key role in Alzheimer disease synaptic dysfunction in vivo. *Cell Death Dis.* 2014;5:e1019.
- Pollak DD, Scharl T, Leisch F, et al. Strain-dependent regulation of plasticity-related proteins in the mouse hippocampus. *Behav Brain Res.* 2005;165:240-246.
- Takizawa H, Hiroi N, Funahashi A. Mathematical modeling of sustainable synaptogenesis by repetitive stimuli suggests signaling mechanisms in vivo. *PLoS One.* 2012;7:e51000.
- Mizui T, Sekino Y, Yamazaki H, et al. Myosin II ATPase activity mediates the long-term potentiation-induced exodus of stable F-actin bound by Drebrin A from dendritic spines. *PLoS One.* 2014;9:e85367.
- Tanabe K, Yamazaki H, Inaguma Y, et al. Phosphorylation of drebrin by cyclin-dependent kinase 5 and its role in neuronal migration. *PLoS One.* 2014;9:e92291.
- Mizui T, Kojima N, Yamazaki H, Katayama M, Hanamura K, Shirao T. Drebrin E is involved in the regulation of axonal growth through actin-myosin interactions. *J Neurochem.* 2009;109:611-622.
- Dun XP, Bandeira de Lima T, Allen J, Geraldo S, Gordon-Weeks P, Chilton JK. Drebrin controls neuronal migration through the formation and alignment of the leading process. *Mol Cell Neurosci.* 2012;49:341-350.
- Aoki C, Sekino Y, Hanamura K, et al. Drebrin A is a postsynaptic protein that localizes in vivo to the submembranous surface of dendritic sites forming excitatory synapses. *J Comp Neurol.* 2005;483:383-402.
- Counts SE, He B, Nadeem M, Wu J, Scheff SW, Mufson EJ. Hippocampal Drebrin loss in mild cognitive impairment. *Neurodegener Dis.* 2012;10:216-219.
- Rao JS, Rapoport SI, Kim HW. Altered neuroinflammatory, arachidonic acid cascade and synaptic markers in postmortem Alzheimer's disease brain. *Transl Psychiatry.* 2011;1:e31.

23. Cho IH, Lee MJ, Kim DH, et al. SPIN90 dephosphorylation is required for cofilin-mediated actin depolymerization in NMDA-stimulated hippocampal neurons. *Cell Mol Life Sci.* 2013;70:4369-4383.
24. Menon S, Gupton SL. Building blocks of functioning brain: cytoskeletal dynamics in neuronal development. *Int Rev Cell Mol Biol.* 2016;322:183-245.
25. Moy SS, Nadler JJ, Young NB, et al. Mouse behavioral tasks relevant to autism: phenotypes of 10 inbred strains. *Behav Brain Res.* 2007;176:4-20.
26. Jung D, Hwang YJ, Ryu H, Kano M, Sakimura K, Cho J. Conditional knockout of Cav2.1 disrupts the accuracy of spatial recognition of CA1 place cells and spatial/contextual recognition behavior. *Front Behav Neurosci.* 2016;10:214.
27. Arqué G, Fotaki V, Fernández D, Martínez de Lagrán M, Arbonés ML, Dierssen M. Impaired spatial learning strategies and novel object recognition in mice haploinsufficient for the dual specificity tyrosine-regulated kinase-1A (Dyrk1A). *PLoS One.* 2008;3:e2575.
28. Paxinos G, Franklin KBJ. *The Mouse Brain in Stereotaxic Coordinates.* 2nd edition. Cambridge, MA: Academic Press; 2001.
29. Esposito Z, Belli L, Toniolo S, Sancesario G, Bianconi C, Martorana A. Amyloid  $\beta$ , glutamate, excitotoxicity in Alzheimer's disease: are we on the right track? *CNS Neurosci Ther.* 2013;19:549-555.
30. Xu ZQ, Zhang LQ, Wang Q, et al. Aerobic exercise combined with antioxidative treatment does not counteract moderate- or mid-stage Alzheimer-like pathophysiology of APP/PS1 mice. *CNS Neurosci Ther.* 2013;19:795-803.
31. Clarke LE, Barres BA. Emerging roles of astrocytes in neural circuit development. *Nat Rev Neurosci.* 2013;14:311-321.
32. Sirko S, Irmiler M, Gascón S, et al. Astrocyte reactivity after brain injury: the role of galectins 1 and 3. *Glia.* 2015;63:2340-2361.
33. Harris JL, Choi IY, Brooks WM. Probing astrocyte metabolism in vivo: proton magnetic resonance spectroscopy in the injured and aging brain. *Front Aging Neurosci.* 2015;7:202.
34. Chimura T, Launey T, Yoshida N. Calpain-mediated degradation of Drebrin by excitotoxicity in vitro and in vivo. *PLoS One.* 2015;10:e0125119.
35. Mitsuyama F, Futatsugi Y, Okuya M, et al. Amyloid beta: a putative intra-spinal microtubule-depolymerizer to induce synapse-loss or dendritic spine shortening in Alzheimer's disease. *Ital J Anat Embryol.* 2009;114:109-120.
36. Scheff SW, Price DA, Ansari MA, et al. Synaptic change in the posterior cingulate gyrus in the progression of Alzheimer's disease. *J Alzheimers Dis.* 2015;43:1073-1090.
37. Yamamoto M, Urakubo T, Tominaga-Yoshino K, Ogura A. Long-lasting synapse formation in cultured rat hippocampal neurons after repeated PKA activation. *Brain Res.* 2005;1042:6-16.
38. Bliss TV, Collingridge GL. A synaptic model of memory: long-term potentiation in the hippocampus. *Nature.* 1993;361:31-39.
39. Holscher C, eds. *Long-Term Potentiation Induced by Stimulation on the Positive Phase of Theta Rhythm: A Better Model for Learning and Memory?*. Cambridge: Cambridge University Press; 2001:146-167.
40. Tonnies E, Trushina E. Oxidative stress, synaptic dysfunction, and Alzheimer's disease. *J Alzheimers Dis.* 2017;57:1105-1121.
41. Sathya M, Moorthi P, Premkumar P, Kandasamy M, Jayachandran KS, Anusuyadevi M. Resveratrol intervenes in the cholesterol- and isoprenoid-mediated amyloidogenic processing of A $\beta$ PP in familial Alzheimer's disease. *J Alzheimers Dis.* 2016. <https://doi.org/10.3233/JAD-161034>
42. Liu DS, Pan XD, Zhang J, et al. APOE4 enhances age-dependent decline in cognitive function by down-regulating an NMDA receptor pathway in EFAD-Tg mice. *Mol Neurodegener.* 2015;10:7.
43. Minter MR, Moore Z, Zhang M, et al. Deletion of the type-1 interferon receptor in APPSWE/PS1 $\Delta$ E9 mice preserves cognitive function and alters glial phenotype. *Acta Neuropathol Commun.* 2016;4:72.
44. Song N, Zhang L, Chen W, et al. Cyanidin 3-O- $\beta$ -glucopyranoside activates peroxisome proliferator-activated receptor- $\gamma$  and alleviates cognitive impairment in the APP(swe)/PS1( $\Delta$ E9) mouse model. *Biochim Biophys Acta.* 2016;1862:1786-1800.
45. Lim LW, Shrestha S, Or YZ, et al. Tetratricopeptide repeat domain 9A modulates anxiety-like behavior in female mice. *Sci Rep.* 2016;6:37568.
46. Sonego M, Oberoi M, Stoddart J, et al. Drebrin regulates neuroblast migration in the postnatal mammalian brain. *PLoS One.* 2015;10:e0126478.
47. Seo J, Giusti-Rodríguez P, Zhou Y, et al. Activity-dependent p25 generation regulates synaptic plasticity and A $\beta$ -induced cognitive impairment. *Cell.* 2014;157:486-498.
48. Heppner FL, Ransohoff RM, Becher B. Immune attack: the role of inflammation in Alzheimer disease. *Nat Rev Neurosci.* 2015;16:358-372.
49. Lopategui Cabezas I, Herrera Batista A, Pentón Rol G. The role of glial cells in Alzheimer disease: potential therapeutic implications. *Neurologia* 2014;29:305-309.
50. Woo JA, Boggess T, Uhlir C, et al. RanBP9 at the intersection between cofilin and A $\beta$  pathologies: rescue of neurodegenerative changes by RanBP9 reduction. *Cell Death Dis.* 2015;6:1676.
51. Wyss-Coray T, Rogers J. Inflammation in Alzheimer disease—a brief review of the basic science and clinical literature. *Cold Spring Harb Perspect Med.* 2012;2:a006346.
52. Pekny M, Wilhelmsson U, Pekna M. The dual role of astrocyte activation and reactive gliosis. *Neurosci Lett.* 2014;565:30-38.
53. Sajja VS, Hlavac N, VandeVord PJ. Role of Glia in memory deficits following traumatic brain injury: biomarkers of Glia dysfunction. *Front Integr Neurosci.* 2016;10:7.
54. Sochocka M, Diniz BS, Leszek J. Inflammatory response in the CNS: friend or foe? *Mol Neurobiol.* 2016. <https://doi.org/10.1007/s12035-016-0297-1>
55. Gordon-Weeks PR. The role of the drebrin/EB3/Cdk5 pathway in dendritic spine plasticity, implications for Alzheimer's disease. *Brain Res Bull.* 2016;126:293-299.
56. Grintsevich EE, Reisler E. Drebrin inhibits cofilin-induced severing of F-actin. *Cytoskeleton (Hoboken).* 2014;71:472-483.
57. Farah CA, Leclerc N. HMWMAP2: new perspectives on a pathway to dendritic identity. *Cell Motil Cytoskeleton.* 2008;65:515-527.
58. Teng J, Takei Y, Harada A, Nakata T, Chen J, Hirokawa N. Synergistic effects of MAP2 and MAP1B knockout in neuronal migration, dendritic outgrowth, and microtubule organization. *J Cell Biol.* 2001;155:65-76.
59. Sánchez C, Díaz-Nido J, Avila J. Phosphorylation of microtubule-associated protein 2 (MAP2) and its relevance for the regulation of the neuronal cytoskeleton function. *Prog Neurobiol.* 2000;61:133-168.

**How to cite this article:** Liu Y, Xu Y-F, Zhang L, Huang L, Yu P, Zhu H, Deng W, Qin C. Effective expression of Drebrin in hippocampus improves cognitive function and alleviates lesions of Alzheimer's disease in APP (swe)/PS1 ( $\Delta$ E9) mice. *CNS Neurosci Ther.* 2017;23:590–604. <https://doi.org/10.1111/cns.12706>